Available online at www.sciencedirect.com
SCIENCE DIRECT®
Journal of Organometallic Chemistry 690 (2005) 4704–4711
Journal of Organometallic Chemistry
www.elsevier.com/locate/jorganchem

The synthesis and characterization of $Re_3(\mu\text{-}H)_3(CO)_{9-n}(PMe_3)_n(\mu_3\text{-}\eta^2\text{:}\eta^2\text{:}\eta^2\text{-}C_{60})$ ($n = 2, 3$) complexes

Hongkyu Kang [a], Bo Keun Park [a], Md. Arzu Miah [a], Hyunjoon Song [a], David G. Churchill [a], Sangwoo Park [b], Moon-Gun Choi [b], Joon T. Park [a,*]

[a] National Research Laboratory, Department of Chemistry and School of Molecular Science (BK 21), Korea Advanced Institute of Science and Technology, 373-1, Guseong-dong, Yuseong-gu, Daejeon 305-701, Republic of Korea
[b] Department of Chemistry and Molecular Structure Laboratory, Yonsei University, Seoul 120-749, Republic of Korea

Received 27 April 2005; received in revised form 4 July 2005; accepted 12 July 2005
Available online 30 August 2005

Abstract

Treatment of $Re_3(\mu\text{-}H)_3(CO)_9(\mu_3\text{-}\eta^2\text{:}\eta^2\text{:}\eta^2\text{-}C_{60})$ (**1**) with 2.2 equiv. of Me_3NO in the presence of excess PMe_3 in chlorobenzene (CB) gave the bisphosphine-substituted complex 1,2-$Re_3(\mu\text{-}H)_3(CO)_7(PMe_3)_2(\mu_3\text{-}\eta^2\text{:}\eta^2\text{:}\eta^2\text{-}C_{60})$ as two diastereomers, **2a** (major, 38%) and **2b** (minor, 11%). The corresponding reaction of **1** with 3.3 equiv. of Me_3NO, produced the trisphosphine-substituted isomeric product 1,2,3-$Re_3(\mu\text{-}H)_3(CO)_6(PMe_3)_3(\mu_3\text{-}\eta^2\text{:}\eta^2\text{:}\eta^2\text{-}C_{60})$ as two diastereomers, **3a** (major, 37%) and **3b** (minor, 15%). Complexes **2a**–**3b** have been characterized by spectroscopic methods and elemental analyses. Single crystal X-ray diffraction studies were carried out for **2a** and **3b**. The hydrides were confirmed by ^1H NMR spectroscopic method and directly located only for **3a** by X-ray diffraction. The molecular structure of **2a** confirms a face-capping $\mu_3\text{-}\eta^2\text{:}\eta^2\text{:}\eta^2\text{-}C_{60}$ ligand with one axial and one equatorial PMe_3 ligand on adjacent rhenium atoms, whereas that for **3b** exhibits pseudo-*Cs* symmetry with an additional equatorial PMe_3 on the third rhenium atom. Molecular structures for **2b** and **3a** are proposed by axial PMe_3 ligand placement and subsequent equatorial PMe_3 placement, based on earlier observations of facile ligand site-exchange in closely related systems and were verified by ^1H NMR spectroscopic method.

Keywords: Trirhenium-hydrido clusters; Trimethyl phosphine; [60]Fullerene; X-ray structures

1. Introduction

The interaction between metal clusters and a carbon cluster such as C_{60} is one of the most interesting topics in the area of exohedral metallofullerene chemistry [1]. In particular, C_{60}-metal cluster complexes have been dominated by the face-capping cyclohexatriene-like bonding mode, $\mu_3\text{-}\eta^2\text{:}\eta^2\text{:}\eta^2\text{-}C_{60}$. This unique π-bonding nature renders remarkable thermal stability to C_{60}–metal cluster complexes and strong electronic communication between C_{60} and metal centers [2]. Furthermore, the electronic communication between C_{60} and metal clusters can be readily fine-tuned with ligands attached to the metal centers [2a,3]. We have demonstrated that the existing C_{60} bonding modes on the cluster framework can be converted to new modes through modifying the coordination sphere of metal centers to which C_{60} is coordinated [4]. This has led to continued and vigorous studies of C_{60}–metal cluster chemistry in which fullerene tuning is controlled by ligand substitution. A combination of both the donor (phosphine) and acceptor (C_{60}) ligands at one metal framework may give the complex not only a unique thermal stability but also more pronounced electronic, optical and magnetic properties [5]. This substitution

* Corresponding author. Tel.: +82 42 869 2826; fax: +82 42 869 5826.
E-mail address: joontpark@kaist.ac.kr (J.T. Park).

0022-328X/$ - see front matter © 2005 Elsevier B.V. All rights reserved.
doi:10.1016/j.jorganchem.2005.07.052

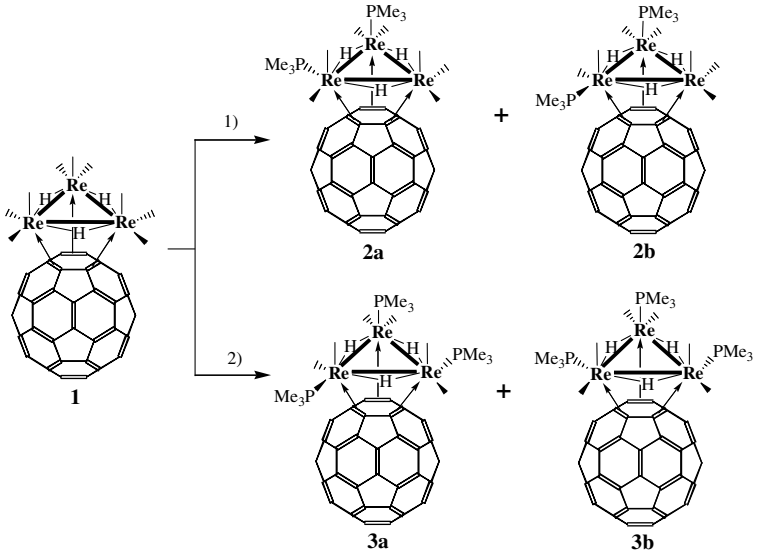

Scheme 1. (1) 2.2 equiv. Me_3NO, PMe_3, CB, reflux, 10 min; (2) 3.3 equiv. Me_3NO, PMe_3, CB, 60 °C, 1 h.

chemistry is helpful both in stabilizing a great variety of C_{60}–metal cluster complexes and in future nano-technological applications of these complexes [6]. Phosphine-substituted C_{60}–metal cluster chemistry has involved the $[Re_3(\mu\text{-}H)_3]$ [3a], $[Os_3]$ [7], $[Ru_5C]$ [8], $[Os_5C]$ [4a], $[Ir_4]$ [9], and $[Rh_6]$ [10] frameworks.

We have previously reported the synthesis and characterization of $Re_3(\mu\text{-}H)_3(CO)_9(\mu_3\text{-}\eta^2\text{:}\eta^2\text{:}\eta^2\text{-}C_{60})$ (**1**) and its derivatives, such as $Re_3(\mu\text{-}H)_3(CO)_8(PPh_3)(\mu_3\text{-}\eta^2\text{:}\eta^2\text{:}\eta^2\text{-}C_{60})$ and $Re_3(\mu\text{-}H)_3(CO)_8(CNCH_2Ph)(\mu_3\text{-}\eta^2\text{:}\eta^2\text{:}\eta^2\text{-}C_{60})$ [3a]. Interestingly, both the PPh_3 and $CNCH_2Ph$ donor ligands occupy axial sites in these trirhenium C_{60} complexes; in contrast, axial isomers have not been isolated for the trimetallic (M = Ru, Os) C_{60} carbonyl clusters. The $Re_3(\mu\text{-}H_3)$ hydride core may result in the additional possibility of selectively delivering hydrogen atoms to the C_{60} moiety. To reflect our ongoing efforts, we report here the syntheses and characterization of tertiary phosphine-substituted stereoisomeric compounds $Re_3(\mu\text{-}H)_3(CO)_{9-n}(PMe_3)_n(\mu_3\text{-}\eta^2\text{:}\eta^2\text{:}\eta^2\text{-}C_{60})$ ($n = 2$, **2a** and **2b**; 3, **3a** and **3b**) from the treatment of **1** with PMe_3, decarbonylated by Me_3NO as shown in Scheme 1. Molecular structures of **2a** and **3b** have been elucidated by X-ray diffraction studies and ligand positions in **2b** and **3a** have been proposed: the first PMe_3 ligand is fixed at the axial position and the remaining PMe_3 ligands are arranged based on an understanding of low energy equatorial site exchange at one metal center in the cluster.

2. Results and discussion

2.1. Synthesis and characterization of *2a, 2b, 3a and 3b*

Decarbonylation of $Re_3(\mu\text{-}H)_3(CO)_9(\mu_3\text{-}\eta^2\text{:}\eta^2\text{:}\eta^2\text{-}C_{60})$ (**1**) with 2.2 equiv. of Me_3NO/MeCN, followed by reaction with PMe_3 in chlorobenzene (CB) at refluxing temperature for 10 min, afforded 1,2-$Re_3(\mu\text{-}H)_3(CO)_7(PMe_3)_2(\mu_3\text{-}\eta^2\text{:}\eta^2\text{:}\eta^2\text{-}C_{60})$ as two diastereomers **2a** (major, 38%) and **2b** (minor, 11%) (Scheme 1). The corresponding reaction of **1** with 3.3 equiv. of Me_3NO/MeCN in the presence of PMe_3 gave 1,2,3-$Re_3(\mu\text{-}H)_3(CO)_6(PMe_3)_3(\mu_3\text{-}\eta^2\text{:}\eta^2\text{:}\eta^2\text{-}C_{60})$ as two diastereomers **3a** (major, 37%) and **3b** (minor 5%).

All four compounds **2a**–**3b** were characterized by IR, NMR, mass spectrometric and elemental analysis, together with single crystal X-ray diffraction studies for **2a** and **3b**. Compounds **2** and **3** are formulated from the molecular ion isotope multiplets (highest peak) m/z 1630 for **2** and 1678 for **3**, respectively, in the FAB^+ mass spectrum and from microanalytical data. Compounds **2a** and **2b** exhibit strong ν(CO) stretches at 2054–1913 cm^{-1}, shifted 30–35 cm^{-1} to lower energy compared to **1**, pointing to an electronic effect from the presence of PMe_3 ligand. Similarly, IR spectra of **3a** and **3b** exhibit stretching bands for terminally bonded carbonyl ligands at considerably lower frequency (2039–1869 cm^{-1}) than for **1**, due to the enhanced electron donation by the three phosphine ligands. Structures of **2b** and **3a** are proposed based on fixing the first PMe_3 ligand axially. Activation parameters (E_a) for the interconversion of $Re_3(\mu\text{-}H)_3(CO)_{11}L$ axial to equatorial are 86(4) kJ mol^{-1} for $L = PPh_3$ and 89(1) kJ mol^{-1} for $L = PPh_2Me$ [11]. Furthermore, axial-to-equatorial isomerization was not observed in either $Re_3(\mu\text{-}H)_3(CO)_8(PPh_3)(\mu_3\text{-}\eta^2\text{:}\eta^2\text{:}\eta^2\text{-}C_{60})$ or $Re_3(\mu\text{-}H)_3(CO)_8(CNCH_2Ph)(\mu_3\text{-}\eta^2\text{:}\eta^2\text{:}\eta^2\text{-}C_{60})$ [3a]. However, activation barriers ($\Delta G^{\ddagger}$) for equatorial site exchanges between PPh_3 and CO ligands for $Os_3(CO)_{9-n}(PPh_3)_n(\mu_3\text{-}\eta^2\text{:}\eta^2\text{:}\eta^2\text{-}C_{60})$ ($n = 1$–3) were reported to be in the range of 47–62 kJ mol^{-1} [12]. This relatively low energy equatorial site exchanges on the same metal found in osmium

complexes may account for the remaining PMe_3 ligand assignments in **2b** and **3a** (Scheme 1). The other possible structure with *cis*, *cis*-equatorial PMe_3 ligands for **3a** was precluded due to expected steric repulsions between PMe_3 ligands. Compounds **2a**, **2b** and **3a**, **3b** are in equilibrium, respectively. Equilibrium constants ([**b**]/[**a**]), 0.09 (35 °C) for **2** and 0.43 for (40 °C) for **3**, were obtained by time-resolved integration of the hydride resonances in the ^1H NMR spectra. However, the equilibration is slow enough at room temperature not only to isolate isomers by use of preparative TLC but also to characterize them by routine NMR spectroscopic methods.

The aliphatic region of the ^1H NMR spectrum of the major isomer **2a** contains two doublets at δ 2.43 and 2.20 with an intensity ratio of 1:1, consistent with 18 PMe_3 protons. The hydride region containing one doublet of doublets and two doublets confirms the presence and nature of the hydride ligands, from which phosphine positioning is inferred (Fig. 1(a)). The doublet of doublet signal at δ −14.28 accounts for the hydride (H_a) that couples to two neighboring non-equivalent phosphorus nuclei ($J_{PH} = 15.2$ Hz and $J_{PH} = 17.6$ Hz), both phosphines are *cis* to the hydride ligand. The magnitude of the coupling constant, i.e., $J_{PH} = 15.2$ Hz, is exactly the same as in $Re_3(\mu\text{-}H)_3(CO)_8(PPh_3)(\mu_3\text{-}\eta^2{:}\eta^2{:}\eta^2\text{-}C_{60})$ (*cis*-coupling, $J_{PH} = 15.2$), in which the PPh_3 ligand occupies the axial position on the Re atom [3a]. The two doublets at δ −14.61 ($J_{PH} = 18.4$ Hz), and −15.16 ($J_{PH} = 6.8$ Hz) are assigned to H_b and H_c, respectively, (Fig. 1(a)). H_b is assigned to the hydride that couples to the axial phosphorus nucleus (*cis*-coupling, $J_{PH} = 18.4$ Hz), and H_c is assigned to the hydride that couples to the equatorial phosphorus nucleus (*trans*-coupling, $J_{PH} = 6.8$ Hz), since large coupling constants are from *cis*-coupling in these rhenium clusters. In particular, relatively large *cis*-coupling constants were previously observed for rhenium complexes such as *ax*-$Re_3(\mu\text{-}H)_3(CO)_{11}(PMe_3)$ (*cis*-coupling, $J_{PH} = 16$ Hz) [11] and eq,eq-$[Re_3(\mu\text{-}H)_2(CO)_{10}(PPh_3)_2]^-$ (*cis*-coupling, $J_{PH} = 24$ Hz)[13], although the *trans*-coupling is commonly known to be larger than the *cis*-coupling in P–M–H complexes. The ^{31}P $\{^1H\}$ NMR spectrum of **2a** contains singlets at δ −37.0 and δ −42.7, with an intensity ratio of 1:1 for the two non-equivalent ^{31}P atoms. In the case of the minor isomer **2b**, the hydride region of the spectrum (Fig. 1(b)) displayed a doublet of doublets centered at δ −14.86 corresponding to H_a undergoing *cis*-coupling ($J_{PH} = 16.8$ Hz) as well as *trans*-coupling ($J_{PH} = 2.4$ Hz) in addition to two doublets at δ 2.46 and 2.24 in a 1:1 ratio for the methyl protons of PMe_3. The two doublets at δ −14.33 and −15.03 are assignable to H_b and H_c, respectively, coupled (*cis*-couplings, $J_{PH} = 17.6$ Hz and $J_{PH} = 16.8$ Hz) to neighboring but non-equivalent ^{31}P atoms. The ^{31}P $\{^1H\}$ NMR of **2b** exhibited two singlets at δ −39.2 and −45.8 for the two ^{31}P atoms, one axially coordinated to one Re atom and the other equatorially bonded to a second Re atom.

The aliphatic region of ^1H NMR spectrum for **3a** contains three doublets at δ 2.42, 2.20 and 2.17 with an intensity ratio of 1:1:1 accounting for 27 protons of the three PMe_3 ligands. The hydride region (Fig. 2(a)) exhibits three doublets of doublets at δ −13.83 (*cis*-couplings, $J_{PH} = 16.4$ and 17.2 Hz), −14.50 (*cis*, $J_{PH} = 16.8$ Hz and *trans*, 3.2 Hz), and −14.62 (*cis*, $J_{PH} = 18.0$ Hz and *trans*, 4.0 Hz) due to H_b, H_a, and H_c, respectively. Whereas, the ^1H NMR spectrum of **3b** (Fig. 2(b)) indicates a pseudo *Cs* symmetry and displayed a doublet of doublets at δ −13.90 (*cis*-couplings, $J_{PH} = 18.0$ and 15.0 Hz) due to two magnetically equivalent hydride ligands of H_a and

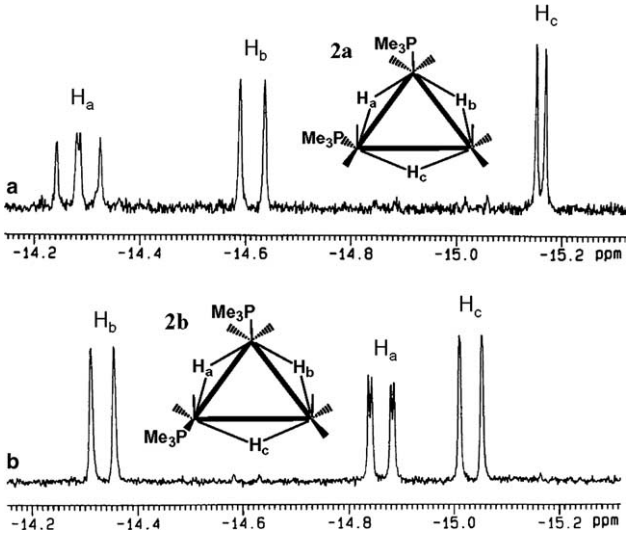

Fig. 1. The ^1H NMR spectrum (hydride region, $CDCl_3$) of compounds: (a) **2a** and (b) **2b**. Carbonyl and C_{60} ligands are omitted for clarity.

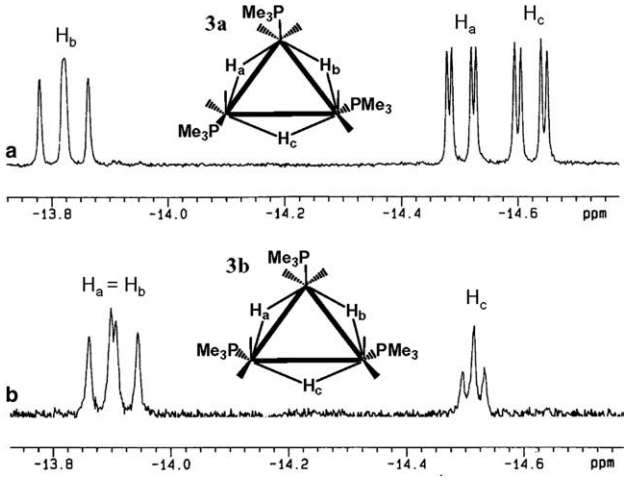

Fig. 2. The ^1H NMR spectrum (hydride region, $CDCl_3$) of compounds: (a) **3a** and (b) **3b**. Carbonyl and C_{60} ligands are omitted for clarity.

H_b, and a triplet at δ −14.51 (*trans*, $J_{PH} = 7.4$ Hz) for H_c due to two magnetically equivalent phosphine ligands giving an intensity ratio of 2:1. These assignments are also consistent with the unusual observation of the larger *cis*-coupling than the *trans*-coupling in **2a** and **2b**. The $^{31}P\{^1H\}$ NMR spectrum of **3a** indicates three well-resolved singlets at δ − 38.3, −44.6 and −45.1 for the three ^{31}P nuclei with an equal intensity ratio of 1:1:1. On the other hand, there are two singlets at δ −36.8 and −43.3 with an intensity ratio of 1:2 for the three ^{31}P nuclei of the minor isomer **3b**.

D'Alfonso and cowokers reported that the substitution of the axially coordinated NCMe in $Re_3(\mu\text{-}H)_3(CO)_{11}(NCMe)$ by various phosphines (L = PPh_3, PMe_3 and $P(OMe)_3$) produces axial derivatives of the form $Re_3(\mu\text{-}H)_3(CO)_{11}L$, which then transform reversibly into the dominant equatorial isomers [11]. Among these phosphine derivatives, however, crystallographic data were obtained for equatorial $Re_3(\mu\text{-}H)_3(CO)_{11}(PPh_3)$ isomer only [14]. Crystal structures of disubstituted $Re_3(\mu\text{-}H)_3(CO)_{10}L_2$ are not known, although anionic $[NEt_4][Re_3(\mu\text{-}H)_2(CO)_{10}(PPh_3)_2]$ has been structurally characterized, in which two phosphines occupy non-equivalent equatorial coordination sites in *cis*, *trans* stereochemistry [13]. In $Re_3(\mu\text{-}H)_3(CO)_8(tedip)_2$ (tedip = $(EtO)_2POP(OEt)_2$), however, four axial sites are occupied by the two bidentate tedip ligands on the opposite side of the rhenium triangle [15]. The $Re_3(\mu\text{-}H)_3(CO)_9$ fragment can be likened to the isoelectronic $Os_3(CO)_9$ moiety in regards to the mode of carbonyl substitution by phosphines. For the reaction of $Os_3(CO)_{12-n}(NCMe)_n$ ($n = 1$–3) with phosphines, the products contain all the phosphine ligands in equatorial positions, while the sterically less demanding leaving group MeCN is axially coordinated. For all the phosphine-substituted triangular clusters of the iron triad, axial isomers have not been isolated due to steric reasons [16]. Similarly, a propeller-like geometry is adopted for the phosphine ligands at equatorial positions in $Os_3(CO)_{9-n}(PPh_3)_n(\mu_3\text{-}\eta^2\text{:}\eta^2\text{:}\eta^2\text{-}C_{60})$ ($n = 1, 2, 3$). On the other hand, in our C_{60} trirhenium complexes of $Re_3(\mu\text{-}H)_3(CO)_8(CNCH_2Ph)(\mu_3\text{-}\eta^2\text{:}\eta^2\text{:}\eta^2\text{-}C_{60})$ [3a], **2a**, and **3b**, axial isomers have been characterized by X-ray crystallography (vide infra). The replacement of axially bound MeCN ligands by PMe_3 groups from intermediates $Re_3(\mu\text{-}H)_3(NCMe)_n(CO)_{9-n}(\mu_3\text{-}\eta^2\text{:}\eta^2\text{:}\eta^2\text{-}C_{60})$ ($n = 2, 3$) (although they are not isolated but believed to be produced in situ during the course of reaction) give rise to the mixture of axial-equatorial products. This difference between $[Os_3]$ and $[Re_3(\mu\text{-}H)_3]$ can be attributed to bridging hydrides [17] which results in: (a) longer metal–metal distances, that relieve crowding between the axial carbonyls and P atom substituents, and (b) smaller L_{eq}–M–L_{eq} angles due to six coordination, that increase inter-ligand repulsion for equatorially coordinated bulky ligands (vide infra).

In the case of a single donor ligand, an axial preference of ligands in all the C_{60} rhenium complexes could be explained by both steric and electronic reasons. Equatorial sites at each rhenium center are sterically very congested with six-coordination, and the intramolecular axial interaction is diminished by the lengthening of the Re–Re bonds due to the bridging hydrides as mentioned above [18]. Donor ligands such as PPh_3, PMe_3, and $CNCH_2Ph$ coordinated *trans* to a hydride ligand (equatorial site) are electronically disfavored with respect to those *trans* to an electron-withdrawing C_{60} ligand (axial site) [17]. With the first PMe_3 ligand placed

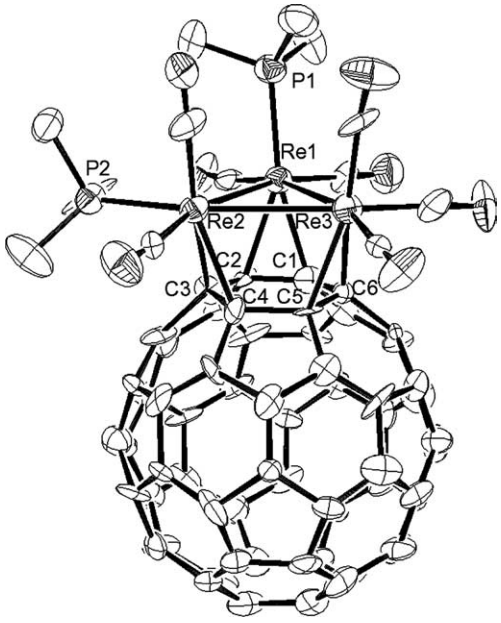

Fig. 3. Molecular structure of **2a** with 50% thermal ellipsoid probability.

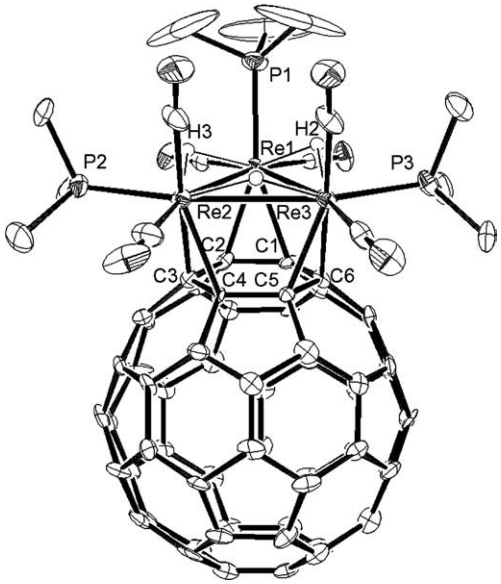

Fig. 4. Molecular structure of **3b** with 50% thermal ellipsoid probability.

axially, the second and third PMe_3 groups prefer equatorial coordination to avoid inter-ligand axial–axial steric collision.

2.2. X-ray crystal structures of **2a** and **3b**

The overall molecular geometry and the atomic labeling scheme of **2a** and **3b** are depicted in Figs. 3 and 4, respectively. Selected interatomic distances and angles for **2a** and **3b** are listed in Tables 1 and 2, respectively.

Compound **2a** contains seven carbonyls, three hydrides, two trimethylphosphine groups, and one C_{60} ligand. One PMe_3 is axially bound to the Re(1) atom, whereas the other is equatorially coordinated to the Re(2) atom. Compound **3b** possesses six carbonyls, three hydrides, three PMe_3 groups, and a C_{60} ligand. It has a mirror plane passing through Re(1) and bisecting the Re(2)–Re(3) bond. Among the three phosphine ligands, one PMe_3 is coordinated to Re(1) in an axial position and lies in this mirror plane. The axial PMe_3 ligand at the Re(1) atom and the two axial carbonyls on the Re(2) and Re(3) atoms are parallel and lie above the Re_3 plane. The two PMe_3 ligands are coordinated to Re(2) and Re(3) at equatorial sites, respectively, in *trans* positions. There are slight variations in the Re–Re bond

Table 1
Selected interatomic distances (Å) and angles with Esd's for **2a**

Bond distances	
(A) Metal–metal distances	
Re(1)–Re(2)	3.217(1)
Re(1)–Re(3)	3.234(1)
Re(2)–Re(3)	3.198(1)
(B) Metal–carbon (C_{60}) distances	
Re(1)–C(1)	2.29(2)
Re(2)–C(3)	2.19(2)
Re(3)–C(5)	2.30(2)
Re(1)–C(2)	2.27(2)
Re(2)–C(4)	2.28(2)
Re(3)–C(6)	2.30(2)
(C) Distances within the C_{60} ligand	
C(1)–C(2)	1.41(3)
C(3)–C(4)	1.30(3)
C(5)–C(6)	1.42(3)
C(2)–C(3)	1.51(3)
C(4)–C(5)	1.55(3)
C(1)–C(6)	1.50(2)
(D) Metal–phosphorus distances	
Re(1)–P(1)	2.429(6)
Re(2)–P(2)	2.416(6)
Bond angles	
(A) Intermetallic angles	
Re(1)–Re(2)–Re(3)	60.55(3)
Re(3)–Re(1)–Re(2)	59.45(3)
Re(2)–Re(3)–Re(1)	60.01(3)
(B) Angles involving metal-coordinated carbon in C_{60}	
C(1)–C(2)–C(3)	118(2)
C(3)–C(4)–C(5)	122(2)
C(5)–C(6)–C(1)	119(1)
C(2)–C(3)–C(4)	122(2)
C(4)–C(5)–C(6)	117(2)
C(6)–C(1)–C(2)	121(2)
(C) Metal–metal–phosphorus angles	
P(1)–Re(1)–Re(2)	98.7(2)
P(2)–Re(2)–Re(3)	161.2(2)
P(1)–Re(1)–Re(3)	102.6(2)
P(2)–Re(2)–Re(1)	100.6(2)

Table 2
Selected interatomic distances (Å) and angles with Esd's for **3b**

Bond Distance	
(A) Metal–metal distances	
Re(1)–Re(2)	3.235(1)
Re(1)–Re(3)	3.238(1)
Re(2)–Re(3)	3.155(1)
(B) Metal–carbon (C_{60}) distances	
Re(1)–C(1)	2.30(1)
Re(2)–C(3)	2.33(1)
Re(3)–C(5)	2.28(1)
Re(1)–C(2)	2.27(1)
Re(2)–C(4)	2.28(1)
Re(3)–C(6)	2.30(1)
(B) Distances within the C_{60} ligand	
C(1)–C(2)	1.46(2)
C(3)–C(4)	1.42(2)
C(5)–C(6)	1.44(2)
C(2)–C(3)	1.50(2)
C(4)–C(5)	1.48(2)
C(1)–C(6)	1.51(2)
(D) Metal–phosphorus distances	
Re(1)–P(1)	2.402(4)
Re(3)–P(3)	2.398(4)
Re(2)–P(2)	2.398(4)
(E) Metal–hydride distances	
Re(1)–H(2)	1.90(1)
Re(2)–H(1)	1.8(1)
Re(3)–H(1)	1.7(1)
Re(1)–H(3)	1.9(2)
Re(2)–H(3)	2.0(2)
Re(3)–H(2)	1.96(1)
Bond angles	
(A) Intermetallic angles	
Re(1)–Re(2)–Re(3)	60.87(3)
Re(3)–Re(1) Re(2)	58.34(3)
Re(2)–Re(3)–Re(1)	60.79(3)
(B) Angles involving metal-coordinated carbon in C_{60}	
C(1)–C(2)–C(3)	119(1)
C(3)–C(4)–C(5)	122(1)
C(5)–C(6)–C(1)	118(1)
C(2)–C(3)–C(4)	119(1)
C(4)–C(5)–C(6)	121(1)
C(6)–C(1)–C(2)	120(1)
(C) Metal–metal–phosphorus angles	
P(1)–Re(1)–Re(2)	100.4(1)
P(2)–Re(2)–Re(3)	163.2(1)
P(3)–Re(3)–Re(2)	160.2(1)
P(1)–Re(1)–Re(3)	100.7(1)
P(2)–Re(2)–Re(1)	102.5(1)
P(3)–Re(3)–Re(1)	99.7(1)

distances, but the average bond lengths in **2a** of 3.216(1) Å and **3b** of 3.209(1) Å agree well with the related triangular trihydrido-rhenium C_{60} complexes, $Re_3(\mu\text{-}H)_3(CO)_8(CNCH_2Ph)(\mu_3\text{-}\eta^2\text{:}\eta^2\text{:}\eta^2\text{-}C_{60})$ (av. 3.190(1) Å) [3a] and other trihydride bridged compounds such as $Re_3(\mu\text{-}H)_3(CO)_{11}(PPh_3)$ (av. 3.262(12) Å) [14], $Re_3(\mu\text{-}H)_3(CO)_{11}(NCMe)$ (av. 3.258(2) Å) [17], $Re_3(\mu\text{-}H)_3(CO)_{10}(NCMe)_2$ (av. 3.266 Å) [19] and $Re_3(\mu\text{-}H)_3(CO)_9(NCMe)_3$ (av. 3.284(1) Å) [17]. These hydride bridged Re–Re distances are elongated compared to the simple Re–Re single bond length in $Re_2(CO)_{10}$ of 3.02 Å [20].

The bridging hydride ligands for **2a** were not located in the structural analysis. However, they have been located for **3b** on a Fourier difference map. The hydride ligands are located above the Re_3 plane, presumably, due to the steric hindrance between the hydrides and the C_{60} ligand. The average Re–H bond distance of **3b** (1.88(1) Å) is slightly longer than that found for $Re_3(\mu\text{-}H)_3(CO)_8(CNCH_2Ph)(\mu_3\text{-}\eta^2\text{:}\eta^2\text{:}\eta^2\text{-}C_{60})$ (1.810 Å) [3a], $Re_3(\mu\text{-}H)_3(CO)_{11}(PPh_3)$ (1.822(8) Å) [14], $Re_3(\mu\text{-}H)_3(CO)_{11}(NCMe)$ (1.83(21) Å) [17], and $Re_3(\mu\text{-}H)_3(CO)_9(NCMe)_3$ (1.80(7) Å) [17]. The C_{60} ligand in both compounds is coordinated to the Re_3 triangle in a typical face-capping $\mu_3\text{-}\eta^2\text{:}\eta^2\text{:}\eta^2\text{-}C_{60}$ fashion, observed in a variety of cluster frameworks [21].

All other geometric features are within the expected range. The average C–C bond length at the junction of the 5,6 ring is 1.44(2) Å and at the 6,6 ring junction is 1.392(2) Å for **2a**, while those for the corresponding ring junctions are 1.451(2) Å and 1.401(2) Å for **3b**, respectively. The Re–CO distances range from 1.90(2) to 1.99(2) for **2a**, and from 1.90(2) to 1.94(2) Å for **3b**. The C–O bond lengths lie between 1.11(2) to 1.20(3) Å for **2a** (av. 1.15(3) Å) and 1.13(2) to 1.17(2) Å for **3b** (av. 1.15(2) Å). The average Re–P bond distances in **2a** and **3b** are 2.423(6) and 2.400(4) Å, respectively.

3. Concluding remarks

The reaction of **1** with PMe_3 initiated by Me_3NO produces di- and tri-substituted stereoisomeric compounds having the general formula $Re_3(\mu\text{-}H)_3(CO)_{9-n}(PMe_3)_n(\mu_3\text{-}\eta^2\text{:}\eta^2\text{:}\eta^2\text{-}C_{60})$ ($n = 2$, **2a** and **2b**; 3, **3a** and **3b**), depending on the stoichiometry of Me_3NO. Single crystal X-ray structures were obtained for **2a** and **3b**. Molecular structures for **2b** and **3a** are proposed based on fixing the first PMe_3 ligand at the axial position and earlier observations of low energy equatorial site exchanges in closely related systems, and were verified by ^1H NMR spectroscopic method. The electrochemical studies of **2** and **3**, however, were not possible due to fluxionality of these complexes in solution during the course of cyclic voltammetric measurements. Nevertheless, in the light of the paucity of studies and structural information of C_{60}-substituted rhenium clusters, our work serves to better understand and appreciate the structure and dynamics of these systems.

4. Experimental

4.1. Materials

All reactions were carried out under a nitrogen atmosphere with use of standard Schlenk techniques. Solvents were dried over the appropriate drying agents and distilled immediately before use. C_{60} (99.5%, SES Research), $Re_2(CO)_{10}$ (98%, Strem), PMe_3 (99%, Aldrich) were used without further purification. Anhydrous trimethylamine N-oxide (m.p. 225–230 °C) was obtained from $Me_3NO \cdot 2H_2O$ (98%, Aldrich) by sublimation (3 times) at 90–100 °C under vacuum. $Re_3(\mu\text{-}H)_3(CO)_9(\mu_3\text{-}\eta^2\text{:}\eta^2\text{:}\eta^2\text{-}C_{60})$ was prepared according to the literature method [3a]. Preparative thin-layer chromatography (TLC) plates were produced with GF254 silica gel (type 60, E. Merck).

4.2. Physical measurements

Infrared spectra were obtained on a Bruker EQUINOX-55 FT-IR spectrophotometer. ^1H NMR (400 MHz) spectra were recorded on a Bruker AVANCE-400 spectrometer and $^{31}P\{^1H\}$ NMR (122 MHz) spectrum were recorded on a Bruker AM-300 spectrometer. Positive ion FAB mass spectra (FAB^+) were obtained by the staff of the Korea Basic Science Center and all m/z values were referenced to ^{186}Re. Elemental analyses were provided by the staff of the Energy and Environment Research Center at KAIST.

4.3. Preparation of 1,2-$Re_3(\mu\text{-}H)_3(CO)_7(PMe_3)_2(\mu_3\text{-}\eta^2\text{:}\eta^2\text{:}\eta^2\text{-}C_{60})$ (2)

To a cholorobenzene solution (50 ml) of **1** (30 mg, 0.0195 mmol), excess PMe_3 was added via syringe at 0 °C. Then anhydrous Me_3NO (2.2 equiv., 2.9 mg, 0.0385 mmol) in MeCN (1 ml) was added dropwise to the solution over ca. 10 min. The resulting reaction mixture was allowed to warm to room temperature for 30 min and subsequently heated to reflux for 10 min. Evaporation of the solvent and purification of the residue by preparative TLC (SiO_2, CS_2/CH_2Cl_2, 4:1) at ca. 5 °C in the refrigerator gave two chromatographic bands. The second band gave **2a** (12.1 mg, 0.0074 mmol, 38%, $R_f = 0.6$) as black crystals after recrystallization from CS_2/hexane (1:10) at −20 °C. IR (CS_2): $\nu_{C\equiv O}$ 2043 (s), 1981 (vs), 1961 (w), 1913 (m) cm^{-1}, ^1H NMR ($CDCl_3$): δ 2.43 (d,$J_{PH} = 9.0$ Hz, 9H, CH_3) 2.20 (d, $J_{PH} = 8.9$ Hz, 9H, CH_3), −14.28 (dd, $J_{PH} = 15.2$ Hz, $J_{PH} = 17.6$ Hz, 1H, ReH), −14.61 (d, $J_{PH} = 18.4$ Hz,

1H, ReH), −15.16 (d, $J_{PH} = 6.8$ Hz, 1H, ReH); $^{31}P\{^1H\}$ (CS_2/ext. CD_2Cl_2): δ −37.0 (s), −42.7 (s). MS (FAB^+) m/z 1630 [M^+]. Anal. Calc. for $C_{73}H_{21}P_2O_7Re_3$: C, 53.77; H, 1.30. Found: C, 53.83; H, 1.36%. The first moving band afforded **2b** (3.5 mg, 0.0021 mmol, 11%, $R_f = 0.75$) as a brown solid after recrystallization in CS_2/hexane (1:10) at −20 °C. IR (CS_2): $\nu_{C=O}$ 2054 (w), 2039 (s), 1988 (s), 1976 (vs), 1946 (w), 1919 (m) cm^{-1}; ^1H NMR ($CDCl_3$): δ 2.46 (d, $J_{PH} = 9.1$ Hz, 9H, CH_3), 2.24 (d, $J_{PH} = 9.0$ Hz, 9H, CH_3), −14.33 (d, $J_{PH} = 17.6$ Hz, 1H, ReH), −14.86 (dd, $J_{PH} = 16.8$ Hz, $J_{PH} = 2.4$ Hz, 1H, ReH), −15.03 (d, $J_{PH} = 16.8$ Hz, 1H, ReH); $^{31}P\{^1H\}$ (CS_2/ext. CD_2Cl_2): δ −39.2 (s), −45.8 (s). MS (FAB^+) m/z 1630 [M^+]. Anal. Calc. for $C_{73}H_{21}P_2O_7Re_3$: C, 53.77; H, 1.30. Found: C, 54.12; H, 1.37%.

4.4. Preparation of 1,2,3-$Re_3(\mu\text{-}H)_3(CO)_6(PMe_3)_3(\mu_3\text{-}\eta^2\text{:}\eta^2\text{:}\eta^2\text{-}C_{60})$ (3)

Applying the same procedure as that for **2**, a mixture of **1** (30 mg, 0.0195 mmol), excess PMe_3 and anhydrous Me_3NO (3.3 equiv., 4.8 mg, 0.0638 mmol) was heated at 60 °C for 1 h and following the similar workup and chromatographic separation as in **2** two chromatographic bands were obtained. The faster moving band gave **3a** (12.2 mg, 0.0073 mmol, 37%, $R_f = 0.45$) isolated as a black solid after recrystallization in CS_2/hexane at −20 °C. IR (CS_2): $\nu_{C=O}$ 1985 (vs), 1971 (vs), 1960 (m), 1907 (m) cm^{-1}; ^1H NMR ($CDCl_3$): δ 2.41 (d, $J_{PH} = 9.0$ Hz, 9H, CH_3), 2.20 (d, $J_{PH} = 8.9$ Hz, 9H, CH_3), 2.15 (d, $J_{PH} = 8.9$ Hz, 9H, CH_3) −13.83 (dd, $J_{PH} = 16.4$ Hz, $J_{PH} = 17.2$ Hz, 1H, ReH), −14.50 (dd, $J_{PH} = 16.8$ Hz, $J_{PH} = 3.2$ Hz, 1H, ReH), −14.62 (dd, $J_{PH} = 18.0$ Hz, $J_{PH} = 4.0$ Hz, 1H, ReH); $^{31}P\{^1H\}$ (CS_2/ext. CD_2Cl_2): δ −38.3 (s), −44.6 (s), −45.1 (s); MS (FAB^+) m/z 1678 [M^+]. Anal. Calc. for $C_{75}H_{30}P_3O_6Re_3$: C, 53.66; H, 1.80. Found: C, 53.39; H, 1.92%. The second band corresponds to **3b** (1.5 mg, 0.0009 mmol, 5%, $R_f = 0.32$) isolated as black crystals after recrystallization from CS_2/hexane (1:10) at −20 °C. IR (CS_2): $\nu_{C=O}$ 2039 (w), 1985 (vs), 1971 (vs), 1921 (s), 1901 (m), 1869 (w) cm^{-1}; ^1H NMR ($CDCl_3$): δ 2.39 (d, $J_{PH} = 9.1$ Hz, 9H, CH_3), 2.17 (d, $J_{PH} = 8.8$ Hz, 18H, CH_3), −13.90 (dd, $J_{PH} = 18.0$ Hz, $J_{PH} = 15.0$ Hz, 2H, ReH), −14.51 (t, $J_{PH} = 7.4$ Hz, 1H, ReH); $^{31}P\{^1H\}$ (CS_2/ext. CD_2Cl_2): δ −36.8 (s), −43.3 (s). MS (FAB^+) m/z 1678 [M^+]. Anal. Calc. for $C_{75}H_{30}P_3O_6Re_3$: C, 53.66; H, 1.80. Found: C, 53.46; H, 1.91%.

4.5. X-ray crystallography

Crystals of **2a** and **3b** suitable for X-ray diffraction studies were grown by diffusion of hexane into a CS_2/CH_2Cl_2 solution of **2a**; and evaporation of CS_2 solution of **3b**. Diffraction data were collected on a Siemens SMART diffractometer/CCD area detector. Preliminary orientation matrix and cell constants were determined from three series of ω scans at different starting angles. Each series consisted of 15 frames, collected at scan intervals of 0.3° ω with an exposure time of 10 s per frame. A total of 32,143 and 15,629 data were collected at 293 K for **2a** and **3b**, respectively. These total reflections were corrected for Lorentz and polarization effects, but no correction for crystal decay was applied. Each structure was solved by direct and difference Fourier methods [22] and was refined by full-matrix least-squares methods based on F^2 (SHELX 97) [23]. All non-hydrogen atoms were refined with anisotropic thermal coefficients. Details of relevant crystallographic data are summarized in Table 3.

Table 3
Crystal and structural determination data for **2a** and **3b**

	2a · $2.5CS_2$	**3b** · $2CS_2$
Formula	$C_{73}H_{18}Re_3O_7P_2 \cdot 2.5CS_2$	$C_{75}H_{30}Re_3O_6P_3 \cdot 2CS_2$
F_w	1817.74	1830.76
Crystal system	Monoclinic	Triclinic
Space group	$P2_1/n$	$P\bar{1}$
a (Å)	10.0278(8)	10.396(2)
b (Å)	28.965(3)	13.152(3)
c (Å)	19.062(2)	21.356(4)
α (°)	90	82.72(3)
β (°)	95.652(2)	82.99(3)
γ (°)	90	78.61(3)
V (Å^3)	5509.6(8)	2825(1)
Z	4	2
D_{calcd} (Mg m^{-3})	2.195	2.152
Temperature (K)	293(2)	293(2)
λ(Mo Kα) (Å)	0.71073	0.71073
μ (mm^{-1})	6.889	6.708
$\theta_{min,max}$ (°)	1.28, 28.02	1.59, 26.54
R_f[a]	0.0894	0.0693
R_w[b]	0.2278	0.1063
Goodness-of-fit	1.082	1.141

[a] $R_f = \sum\|F_o| - |F_c\|/\sum|F_o|$.
[b] $[\sum w(|F_o| - |F_c|)^2 \sum w|F_o|^2]^{1/2}$.

5. Supplementary material

Crystallographic data for the structural analyses have been deposited with the Cambridge Crystallographic Data Centre, CCDC Nos. 265875 (**2a**) and 265876 (**3b**). Copies of this information may be obtained free of charge from The Director, CCDC, 12 Union Road Cambridge, CB2 1EZ, UK (Fax: 0/44 1223 336033; email: deposit@ccdc.cam.ac.uk or www: http://www.ccdc.cam.ac).

Acknowledgment

This work was supported by the National Research Laboratory (NRL) Program of the Ministry of Science and Technology of Korea (MOST).

References

[1] (a) A.L. Balch, M.M. Olmstead, Chem. Rev. 98 (1998) 2123;
(b) A.H.H. Stephens, M.L.H. Green, Adv. Inorg. Chem. 44 (1997) 1.

[2] (a) H. Song, K. Lee, J.T. Park, M.-G. Choi, Organometallics 17 (1998) 4477;
(b) J.T. Park, J.-J. Cho, H. Song, C.-S. Jun, Y. Son, J. Kwak, Inorg. Chem. 36 (1997) 2698.

[3] (a) H. Song, Y. Lee, Z.-H. Choi, K. Lee, J.T. Park, J. Kwak, M.-G. Choi, Organometallics 20 (2001) 3139;
(b) A.J. Babcock, J. Li, K. Lee, J.R. Shapley, Organometallics 21 (2002) 3940.

[4] (a) K. Lee, C.H. Lee, H. Song, J.T. Park, H.Y. Chang, M.-G. Choi, Angew. Chem., Int. Ed. 39 (2000) 1801;
(b) H. Song, K. Lee, C.H. Lee, J.T. Park, H.Y. Chang, M.-G. Choi, Angew. Chem., Int. Ed. 40 (2001) 1500.

[5] (a) T.L. Makarova, B. Sundqvist, R. Höhne, P. Esquinazi, Y. Kopelevich, P. Scharff, V.A. Davydov, L.S. Kashevarova, A.V. Rakhmanina, Nature 413 (2001) 716;
(b) H. Imahori, H. Norieda, H. Yamada, Y. Nishimura, I. Yamazaki, Y. Sakata, S. Fukuzumi, J. Am. Chem. Soc. 123 (2001) 100;
(c) K. Hutchison, J. Schick, Y. Rubin, F. Wudl, J. Am. Chem. Soc. 121 (1999) 5611.

[6] (a) B.I. Yakobson, R.E. Smalley, Am. Sci. 85 (1997) 324;
(b) M.S. Dresselhaus, G. Dresselhaus, P.C. Eklund, Science of Fullerenes and Carbon Nanotubes, Academic Press, San Diego, 1996;
(c) G. Schmid, Clusters and Colloids. From Theory to Applications, VCH, Weinheim, 1994.

[7] J.T. Park, H. Song, J.-J. Cho, M.-K. Chung, J.-H. Lee, I.-H. Suh, Organometallics 17 (1998) 227.

[8] K. Lee, J.R. Shapley, Organometallics 17 (1998) 3020.

[9] (a) G. Lee, Y.-J. Cho, B.K. Park, K. Lee, J.T. Park, J. Am. Chem. Soc. 125 (2003) 13920;
(b) B.K. Park, M.A. Miah, G. Lee, Y.-J. Cho, K. Lee, S. Park, M.-G. Choi, J.T. Park, Angew. Chem., Int. Ed. 43 (2004) 1712.

[10] (a) K. Lee, H. Song, B.S. Kim, J.T. Park, S. Park, M.-G. Choi, J. Am. Chem. Soc. 124 (2002) 2872;
(b) K. Lee, Y.J. Choi, Y.-J. Cho, C.Y. Lee, H.J. Song, C.H. Lee, Y.S. Lee, J.T. Park, J. Am. Chem. Soc. 126 (2004) 9837.

[11] T. Beringhelli, G. D'Alfonso, A.P. Minoja, M. Freni, Inorg. Chem. 30 (1991) 2757.

[12] H. Song, K. Lee, J.T. Park, Y.H. Chang, M.-G. Choi, J. Organomet. Chem. 599 (2000) 49.

[13] T. Beringhelli, G. Ciani, G. D'Alfonso, M. Freni, J. Organomet. Chem. 311 (1986) C51.

[14] C.-Y. Wei, L. Garlaschelli, R. Bau, J. Organomet. Chem. 213 (1981) 63.

[15] D.W. Prest, M.J. Mays, P.R. Raithby, A.G. Orpen, J. Chem. Soc., Dalton. Trans. (1982) 737.

[16] (a) M.I. Bruce, M.J. Liddell, O. Shawakataly, C.A. Hughes, B.W. Skelton, A.H. White, J. Organomet. Chem. 347 (1988) 207;
(b) M.I. Bruce, M.J. Liddell, C.A. Hughes, B.W. Skelton, A.H. White, J. Organomet. Chem. 347 (1988) 157;
(c) M.I. Bruce, M.J. Liddell, C.A. Hughes, J.M. Patrick, B.W. Skelton, A.H. White, J. Organomet. Chem. 347 (1988) 181.

[17] T. Beringhelli, G. D'Alfonso, M. Freni, G. Ciani, M. Moret, A. Sironi, J. Chem. Soc., Dalton Trans. (1989) 1143.

[18] M.R. Churchill, B.G. DeBoer, F.J. Rotella, Inorg. Chem. 15 (1976) 1843.

[19] G. Ciani, A. Sironi, G. D'Alfonso, P. Romiti, M. Freni, J. Organomet. Chem. 354 (1983) C37.

[20] M.R. Churchill, K.N. Amoh, H.J. Wasserman, Inorg. Chem. 20 (1981) 1609.

[21] K. Lee, H. Song, J.T. Park, Acc. Chem. Res. 36 (2003) 78.

[22] G.M. Sheldrick, Acta Crystallogr. A 46 (1990) 467.

[23] G.M. Sheldrick, SHELX97, Program for Crystal Structure Refinement, University of Göttingen, Germany, 1997.